

# On-chip detection of ferromagnetic resonance of a single submicron permalloy strip

M. V. Costache, M. Sladkov, C. H. van der Wal and B. J. van Wees  
*Physics of Nanodevices Group, Materials Science Centre, University of Groningen,  
Nijenborgh 4, 9747 AG Groningen, The Netherlands*

(Dated: September 11, 2018)

## Abstract

We measured ferromagnetic resonance of a single submicron ferromagnetic strip, embedded in an on-chip microwave transmission line device. The method used is based on detection of the oscillating magnetic flux due to the magnetization dynamics, with an inductive pick-up loop. The dependence of the resonance frequency on applied static magnetic field agrees very well with the Kittel formula, demonstrating that the uniform magnetization precession mode is being driven.

Recent discoveries of novel phenomena in mesoscopic systems containing nanomagnets pave the way to new spintronics devices<sup>1,2,3</sup>. Brataas et al.<sup>4</sup> proposed a new application of ferromagnetic resonance (FMR), a so-called spin battery. In such a device, a spin current flows into a paramagnetic metal from its interface with a precessing ferromagnet, which is resonantly driven with an rf magnetic field. A number of experiments<sup>5,6,7,8,9,10</sup>, have been used to measure FMR on thin ferromagnetic films or on ensembles of small ferromagnets. This work measured rf-power transmission or absorption with a coplanar waveguide with ferromagnetic material on top of it, or with ferromagnetic material in a microwave cavity. However, these measurements do not provide enough sensitivity to measure FMR of a single submicron ferromagnetic strip, and cannot be implemented into a lateral multi-terminal device needed for a spin battery device.

We present here experiments which detect FMR of a single submicron permalloy ( $Py = Ni_{80}Fe_{20}$ ) strip, and show that driving of a  $Py$  strip with an external rf field can result in resonant excitation of pure uniform magnetization precession (unlike earlier work on  $Co$  strips<sup>11</sup>, where mainly domain wall resonances and possibly spin wave modes were excited). We studied microwave transmission in a setup with two on-chip coplanar strip waveguides (CSW), see fig. 1. The waveguide with the short at its end is used for generation of a high-amplitude, localized rf magnetic field  $h_{rf}(t)$ . This is used for driving the magnetization of a submicron  $Py$  strip, that is embedded in a small pick-up coil. Oscillations of the magnetic flux in this coil induce a microwave signal in the second CSW, of which the power is detected with a spectrum analyzer<sup>12</sup>. Besides a contribution from the driving field (the source flux), we find that precession of the strip's magnetization gives a contribution (the FMR flux) to the flux in the pick-up coil (superposition of source flux and FMR flux), and that this can be used as a highly sensitive probe for FMR of an individual nanomagnet. Measurements are done by slowly sweeping a static magnetic field  $H_0$  applied along the  $Py$  strip and perpendicular to  $h_{rf}$ , while the generated power at the applied rf frequency was measured by a spectrum analyzer<sup>12</sup>. All the measurements are done at room temperature.

Note, however, that symmetry arguments predict that this type of FMR signals should be zero for our geometry. Upon precession, the magnetization has oscillating components transverse to its equilibrium direction (parallel to the strip's easy axis). For these, the component in the device plane does nominally not result in field lines that pierce the loop. For the out-of-plane component, the flux coming out of the top surface of the strip exactly equals

the flux piercing the surrounding sample plane, and the field falls off rapidly with increasing distance from the strip. Consequently, also this component does not cause a flux in the loop if the loop's boundary is assumed to coincide exactly with the strip's central axis. Our FMR signals are due to deviations from these exact symmetries, which are hard to quantify for devices that we can realize at this stage. Based on the details of our geometry (fig. 1b), we believe that the non-zero flux coupling is dominated by the out-of-plane component.

The devices were fabricated by evaporating a *Py* strip (25 nm thick,  $0.3 \times 3 \mu\text{m}^2$  lateral size) at 2.5  $\mu\text{m}$  distance from the shorted-end of the CSW, and connecting it with *Cu* leads (80 nm thick) to the other CSW. For *Py* and *Cu* e-beam lithography and lift-off was used. The CSW structures were made of *Au* (300 nm thick) by means of optical lithography on a lightly doped silicon wafer with a 500 nm thermal oxide surface layer. The two CSW are designed to have 50  $\Omega$  impedance<sup>13</sup> and connected by means of microwave picoprobes to the rf signal generator and spectrum analyzer. For all measurements the output power of the signal generator was set at 20 dBm (100 mW), the power that reaches the sample, however, is reduced by a few dB.

Figure 2 shows a typical output signal as a function of the static magnetic field ( $H_0$ ), taken for an applied rf frequency of 8 GHz. Two well defined 20  $\mu\text{V}$  dips at  $H_0 = \pm 80 \text{ mT}$  are observed on top of a few mV background. By measuring the transmitted power on a chip without the ferromagnetic strip, it was found that the background signal is unrelated to FMR, and due to a parasitic capacitive coupling between the two CSW (also discussed later).

The inset of Fig. 2 shows the position of the dip for different frequencies of the rf field as a function of the static applied field. The squares correspond to the experimental data, while the solid line is a fit with the Kittel formula for the uniform precession mode<sup>14</sup>:  $\omega_0^2 = \gamma^2 H_0 (H_0 + M_S)$ , where  $\gamma$  is the gyromagnetic ratio. From the fit, the saturation magnetization of the *Py* strip was found to be about  $\mu_0 M_S = 1 \text{ T}$  and the gyromagnetic ratio  $\gamma = 176 \text{ GHz/T}$ , consistent with earlier reports<sup>7</sup>. The excellent fit demonstrates that the magnetization vector of the *Py* strip was driven in the uniform precession mode.

The amplitude of the FMR signature was measured as a function of the amplitude of the rf driving field at 9 GHz (fig. 3), showing a linear dependence. The magnetization precession around the direction of an effective field  $\vec{H}_{eff}$  only results in a small time-dependent component of the magnetization perpendicular to the easy axis  $\vec{M}(t) = m_x(t) \cdot \hat{x} + m_y(t) \cdot \hat{y} + M_S \cdot \hat{z}$

that can be described by the linearized Landau Lifschitz Gilbert (LLG) equation<sup>15</sup>

$$\frac{d\vec{M}}{dt} = -\gamma \left[ \vec{M} \times \vec{H}_{eff} \right] + \frac{\alpha}{M_S} \left[ \vec{M} \times \frac{d\vec{M}}{dt} \right] \quad (1)$$

where  $\alpha$  is the dimensionless Gilbert damping parameter. We solved this equation under the assumption that the strip can be treated as a single domain thin film with a demagnetizing field only in the out-of-plane direction and the crystal anisotropy field is neglected, thus the effective field can be written as  $\vec{H}_{eff} = [-m_y(t) + h(t)] \cdot \hat{y} + H_0 \cdot \hat{z}$ .

The solution of this equation can be presented as the magnetic susceptibility tensor  $\chi_{ij}(\omega)$ . In our particular case only  $\chi_{xy}$  and  $\chi_{yx}$  components are required and since we assume that the out-of-plane component of magnetization dominates the magnetic flux contribution in the loop, the  $\chi_{xy}$  can be excluded from consideration while the  $\chi_{yx}$  has a form (further tensor indices are omitted for simplicity)

$$\chi(\omega) = \gamma M_S \frac{\gamma H_0 + i\omega\alpha}{\omega^2 - \omega_0^2 - i\omega\alpha\gamma(2H_0 + M_S)} \quad (2)$$

In Figure 4(d), we plot the real and imaginary parts of magnetic susceptibility as a function of the static magnetic field ( $H_0$ ) for an rf field of 8 GHz frequency, with  $\gamma = 176 \text{ GHz/T}$ ,  $\mu_0 M_S = 1 \text{ T}$  and  $\alpha = 0.015$ . The imaginary part of  $\chi(\omega)$  describes the out-of-phase magnetization precession. This results in the absorption peak observed in conventional FMR experiments, with a linewidth increasing linearly with frequency and being a function of  $\alpha$ .

Figures 4 (a), (b), (c) show the measured signal around the resonant frequency for three typical rf frequencies 4, 8, and 14 GHz (the squares) from a different sample. We note here that the FMR dip shape changes from a Lorentzian to a more complex shape as the frequency changes. This is due to a parasitic capacitive coupling between the two CSW, meaning that there is an extra contribution to the voltage created by the applied rf field. This can also be understood as a phase shift ( $\varphi$ ) between the voltage created by the source flux and the voltage due to the FMR flux. We fit the the change in voltage observed at resonance using the following function

$$\Delta V(\omega) \propto A(\omega) \cdot (Im[\chi(\omega)] \cdot \cos(\varphi) + Re[\chi(\omega)] \sin(\varphi)) \quad (3)$$

where  $A(\omega)$  depends on the amplitude of the  $h_{rf}$  and on the coupling between the time dependent magnetization and the FMR flux generated by this. With  $A(\omega)$  and  $\varphi$  as fit

parameters, all the measured signals could be fit very well Fig. 4 (a)-(c)). These fits allow us to determine the Gilbert damping parameter, which was found to be  $\alpha = 0.015$ . This value is larger than the value  $\alpha = 0.007$  commonly accepted for a thin film of Py<sup>6,16</sup>. Our higher value can be due to the spatial inhomogeneities of the driving field  $h_{rf}$  and magnetic inhomogeneities at the strip edges<sup>9</sup>, or due to spin pumping<sup>17</sup> from the Py strip into the Cu contacts, as previously measured for a *Cu/Py/Cu* film structure<sup>18</sup>.

Finally, we turn to estimating the precession cone angle, an important parameter for the spin battery proposal. An upper limit can be estimated by assuming that all the rf power from the signal generator leads to rf current in the short at the end of the left CSW. The rf field amplitude driving the strip is then  $\sim 3.8 \text{ mT}$ , which gives a precession cone angle of  $\theta_y \approx h_{RF}/(\alpha M_S) = 13^\circ$ . A lower limit can be obtained from the amplitude  $\Delta V$  of the resonances in the measured ac voltage,  $\theta_y = \Delta V/(\omega \cdot S \cdot M_S)$ , where  $S$  is the effective coupling area of the asymmetries that lead to non-zero flux coupling. If we assume an upper limit for this asymmetry of a reasonable fraction of the strip's surface,  $3000 \times 10 \text{ nm}^2$ , a measured ac voltage amplitude of  $20 \text{ } \mu\text{V}$  at 10 GHz gives a cone angle of  $\theta_y = 2.5^\circ$ . This indicates that the cone angle is a few degrees in our experiment. Further examination and modelling of the asymmetries that lead to non-zero flux coupling and the microwave circuitry is needed for a better understanding of the magnitude of the measured signal.

In summary, we demonstrated the resonant excitation and detection of the ferromagnetic resonance uniform mode of a single submicron ferromagnetic strip, embedded in an on-chip microwave transmission line device. We obtain a precession cone angle of a few degrees, and a Gilbert damping parameter  $\alpha = 0.015$ . These results are promising for further studies on new mechanisms for controlling magnetization and electron spins in lateral nanodevices at high frequencies, as for example the spin battery proposal.

This work was supported by the Dutch Foundation for Fundamental Research on Matter (FOM). We thank S. M. Watts, J. Grollier, G. Visanescu and A. Slachter for contributions to this work, and B. Wolfs and S. Bakker for technical support.

## REFERENCES

---

- <sup>1</sup> S. I. Kiselev, J. C. Sankey, I. N. Krivorotov, N. C. Emley, R. J. Schoelkopf, R. A. Buhrman, and D. C. Ralph, *Nature* **425**, 380 (2003).
- <sup>2</sup> E. Saitoh, H. Miyajima, T. Yamaoka, and G. Tatara, *Nature* **432**, 203 (2004).
- <sup>3</sup> A. A. Tulapurkar, Y. Suzuki, A. Fukushima, H. Kubota, H. Maehara, K. Tsunekawa, D. D. Djayaprawira, N. Watanabe, and S. Yuasa, *Nature* **438**, 339 (2005).
- <sup>4</sup> A. Brataas, Y. Tserkovnyak, G. E. W. Bauer, and B. I. Halperin, *Phys. Rev. B* **66**, 060404 (2002).
- <sup>5</sup> S. Zhang, S. Oliver, N. Israelof, and C. Vittoria, *Appl. Phys. Lett.* **70**, 2756 (1997).
- <sup>6</sup> T. J. Silva, C. S. Lee, T. M. Crawford, and C. T. Rogers, *J. Appl. Phys.* **85**, 7849 (1999).
- <sup>7</sup> F. Giesen, J. Podbielski, T. Korn, M. Steiner, A. van Staa, and D. Grundler, *Appl. Phys. Lett.* **86**, 112510 (2005).
- <sup>8</sup> Y. Ding, T. Klemmer, and T. Crawford, *J. Appl. Phys.* **96**, 2969 (2004).
- <sup>9</sup> B. K. Kuanr, R. Camley, and Z. Celinski, *J. Magn. Magn. Mater.* **286**, 276281 (2005).
- <sup>10</sup> S. E. Russek and S. Kaka, *IEEE Trans. Magn.* **36**, 2560 (2000).
- <sup>11</sup> J. Grollier, M. V. Costache, C. H. van der Wal, and B. J. van Wees, cond-mat/0502197; (Accepted for publication in *J. Appl. Phys.*) (2006).
- <sup>12</sup> The spectrum analyzer measures power, which we convert in a voltage scale assuming 50  $\Omega$  load impedance. To improve the signal-to-noise ratio we employ a frequency locked technique with a 10 Hz spectral bandwidth.
- <sup>13</sup> Gupta, Garg, Bahl, and Bhartia, *Microstrip Lines and Slotlines* (Artech House Publishers, 1996), ISBN 0-89006-766-X.
- <sup>14</sup> C. Kittel, *Introduction to Solid State Physics, Ch. 16* (John Wiley & Sons, 1996).
- <sup>15</sup> T. L. Gilbert, *Phys. Rev.* **100**, 1243 (1955); L. D. Landau, E. M. Lifshitz and L. P. Pitaevski, *Statistical physics, part.2*, (Pergamon, Oxford, 3rd ed. 1980).
- <sup>16</sup> T. Gerrits, T. J. Silva, J. P. Nibargera, and T. Rasing, *J. Appl. Phys.* **96**, 6023 (2005).
- <sup>17</sup> Y. Tserkovnyak, A. Brataas, and G. Bauer, *Phys. Rev. Lett.* **88**, 117601 (2002).
- <sup>18</sup> S. Mizukami, Y. Ando, and T. Miyazaki, *J. Magn. Magn. Mater.* **226**, 1640 (2001).

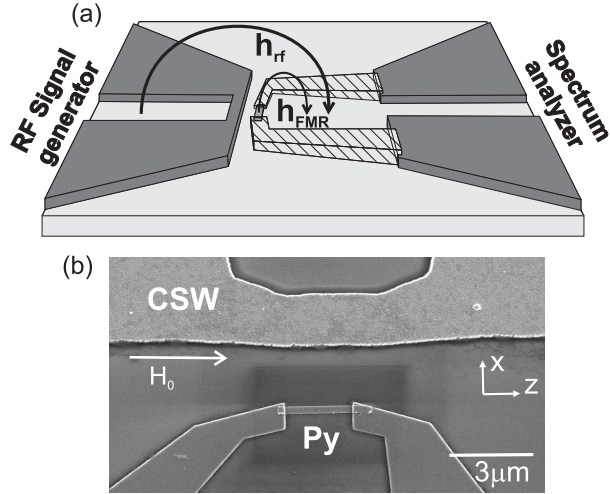


FIG. 1: (a) Schematic diagram of the device. On the left side an rf current is driven through the shorted end of the coplanar strip, which generates an rf magnetic field  $h_{rf}$  (Biot-Savart law). On the right, a loop that contains a submicron Py strip is connected to another coplanar strip. RF power that results from oscillating magnetic flux in this loop is measured with a spectrum analyzer. Magnetization precession of the Py strip contributes a magnetic field  $h_{FMR}$  to the total magnetic field. (b) Scanning electron microscope picture of central part of the device (rotated by  $90^\circ$  with respect to the upper figure).

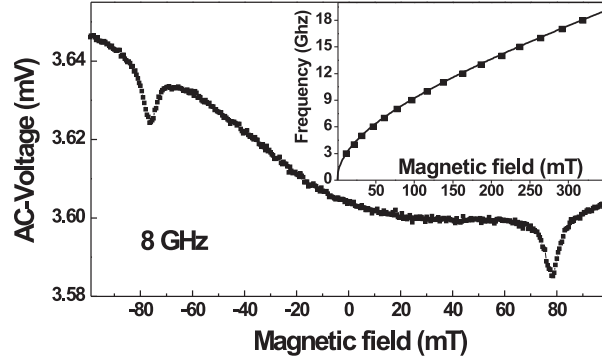


FIG. 2: Measured ac voltage as a function of static magnetic field for an applied rf magnetic field at frequency  $8\text{ GHz}$ . The inset shows the static magnetic field dependence of the resonance frequency, as derived from the dips in the ac voltage versus magnetic field. The squares represent the experimental data, the curve is a fit to the data using the Kittel formula.

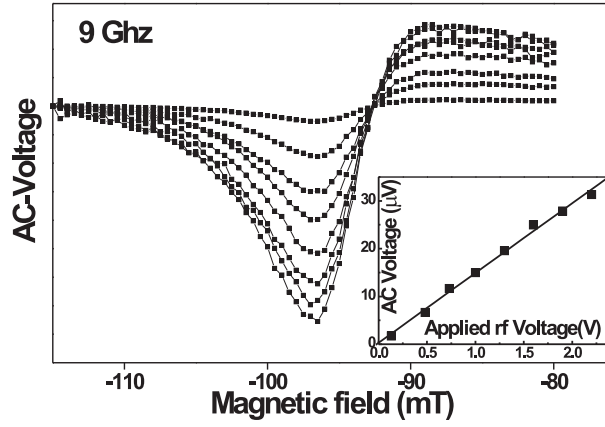


FIG. 3: Measured ac voltage as a function of static magnetic field for a sequence of amplitudes of the rf driving field, at 9 GHz. The inset shows a linear dependence for the amplitude of the FMR signature in the measured ac voltage on the amplitude of the driving field (applied rf voltages scale is used, derived from the applied power assuming  $50 \Omega$  load impedance).

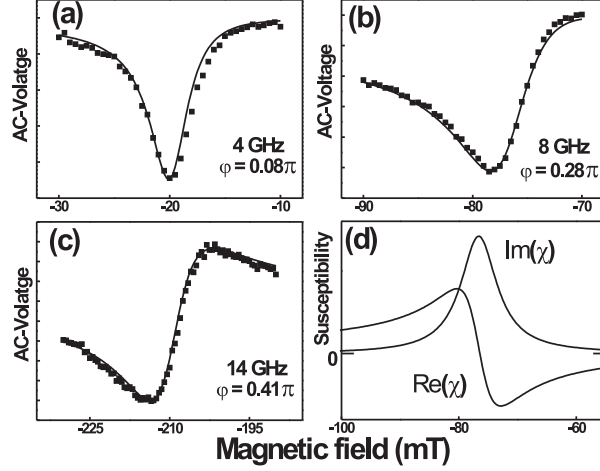


FIG. 4: (a),(b),(c) Measured ac voltage as a function of the static magnetic field, around the resonance position for the frequencies 4 GHz, 8 GHz and 14 GHz, shown by squares. The line is the fit to the data using equation (3) (with the value for  $\varphi$  in the plot). (d) The *real* and the *imaginary* parts of the susceptibility  $\chi$  calculated using equation (2) for rf field frequency 8 GHz,  $\gamma = 176 \text{ GHz/T}$ ,  $M_S = 1 \text{ T}$  and  $\alpha = 0.015$ .